

Critical field behavior and antiband instability under controlled surface electromigration on Si(111)

C. O Coileain, V. Usov,* and I. V. Shvets

Centre for Research on Adaptive Nanostructures and Nanodevices, School of Physics, Trinity College, Dublin 2, Ireland

S. Stoyanov

*Department of Phase Transitions and Crystal Growth, Institute of Physical Chemistry,**Bulgarian Academy of Sciences, BG-1113 Sofia, Bulgaria*

(Received 12 April 2011; revised manuscript received 17 June 2011; published 9 August 2011)

In this study we investigate step bunching and antiband surface instabilities on Si(111). We experimentally study the effects of a controlled electromigration field on the onset of antibands. We analyze the initial stage of antiband formation on step bunched surfaces under conditions of constant temperature of 1270 °C, while systematically varying the applied electromigration field. The relationship between the electromigration field and minimum terrace width required to initiate the antiband formation has been established. Also, we systematically measured values of the critical electromigration field, which is required to initiate the step-bunching process on Si(111) at 1130 °C (regime II) and 1270 °C (regime III). The dependence of the critical field on the mean atomic terrace width has been investigated and discussed.

DOI: [10.1103/PhysRevB.84.075318](https://doi.org/10.1103/PhysRevB.84.075318)

PACS number(s): 68.35.bg, 68.35.Fx, 68.37.Ps, 68.47.Fg

I. INTRODUCTION

The dynamics and evolution of crystalline surfaces have long been the subject of scientific attention,¹ and this has been further stimulated by their recent potential technological applications.^{2,3} The biased diffusion of Si atoms on vicinal Si(111) induced by an applied electric field at temperatures above 860 °C was particularly at the focus due to its complex temperature and electric current orientation dependences.⁴⁻⁶ The electric field applied along the miscut in one particular direction results in closely spaced step bands, each constituting only several atomic heights, while the electric field in the opposite direction causes the atomic steps to develop into several-micrometers-wide flat terraced regions separated by step bunches with a high density of atomic steps and heights of up to hundreds of nanometers. Additionally, this behavior is complicated by the requirement of converse directions of electromigration necessary to induce the step bunching for four specific temperature regimes.⁷ In the temperature regimes I (~850–950 °C) and III (~1200–1300 °C) the step-bunching process is driven by the step-down adatom electromigration. A reversal of the adatom drift is required for regimes II (~1040–1190 °C) and IV (>1300 °C), such that bunching takes place only if the adatoms drift is in the step-up direction.^{4,8} The fundamental mechanism responsible for step bunching is expected to be different for these regimes, with the regimes II and III being the subject of investigation in this paper.

Prolonged annealing, with the dc current driven along the miscut direction, allows the surface morphology to further develop, giving rise to new patterns.⁹ Specifically, the electromigration of adatoms causes steps crossing the terraces to twist until they acquire a reversed alignment and form bands with opposite inclination, as compared to the primary step bunches, close to the terrace edges (antibands) [Fig. 1(a)]. The gradual evolution of the atomic steps crossing the terraces and the creation of sublimation spirals were identified as being responsible for the formation of these antibands in previous experimental studies.⁹ Figure 1(b) demonstrates neighboring terraces containing these features, with the former being the

subject of investigation in this paper. In addition, there have been theoretical studies on the step-bending effects produced by electric currents driven parallel to the atomic steps.¹⁰

Dynamics of atomic steps under the influence of an external electromigration force can be accurately modeled using the generalized Burton-Cabrera-Frank (BCF) theory, which describes step bunching driven by the step-down adatom electromigration observed in temperature regimes I and III.^{5,11} The theory assumes that drifting Si adatoms are unable to cross atomic steps but instead attach to them due to the exchange between the crystal phase and the surface layer of adatoms. An adatom concentration gradient is created across the terrace as a result of adatom electromigration in the down-step direction and the limited rate of adatom attachment at the step edges. In the case of step kinetics limiting sublimation, adatoms arriving at the lower edge cannot be instantly accepted by atomic steps; thus the local adatom concentration is comparatively elevated. The concentration gradient causes the atomic crossing steps to recede along terraces in an uneven manner, i.e., the step velocity near the upper step edge of the terrace is greater than that at the lower edge. This leads to the characteristic long-S-shape deformation of the crossing steps as the terraces widen.

The crossing steps evolve such that a steady state is reached where the variation of the adatom concentration is compensated by the variation of the step curvature.¹² At this point crossing steps have zero net velocity perpendicular to the terraces, while the movement along the terrace is uniform across the whole step. Crossing steps in this state can be recognized by their symmetric S shape and alignment perpendicular to the step bunches. However, the steady state cannot be maintained as the terrace width grows, and this is acknowledged as the onset of the antiband instability. Beyond this point the inner lobes of the S-shaped steps move faster and pass the slower and relatively adatom saturated outer edges of the adjacent steps. Finally, the middle sections of crossing steps align parallel to the step bunches to form an antiband. It has been theoretically shown that this transition occurs when

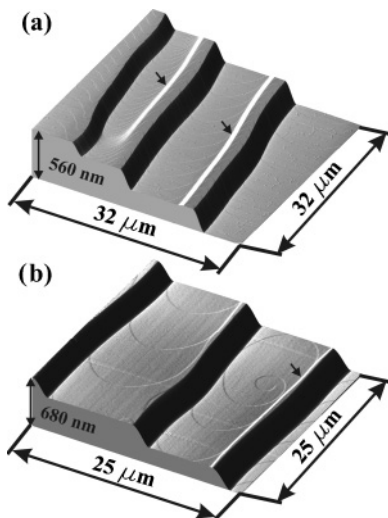


FIG. 1. Surface morphologies created on Si(111) by extended annealing at 1270 °C. (a) AFM image of Si(111) annealed with electric field $E = 3.6$ V/cm, showing 10- (middle terrace) and 14-nm-high antibands located close to terrace edges. Antibands are indicated by arrows. (b) AFM image of Si(111) obtained by annealing with $E = 2.0$ V/cm showing two neighboring terraces, where the antibands developed by sublimation spirals (lower terrace) and bending of crossing steps (upper terrace).

terrace width L and applied electromigration field E satisfy the necessary condition

$$\frac{q_{\text{eff}}EL^2}{\tilde{\beta}a^2} > 2, \quad (1)$$

where q_{eff} is an effective charge of Si adatoms on Si(111), $\tilde{\beta}$ is the atomic step stiffness, and a is the atomic spacing.¹² This clearly proposes that a minimum terrace width is required for the onset of antibands at any given applied electric field. Reduction of the electromigration field results in a widening of the terrace width required to achieve the same stage of crossing-step evolution. Therefore modifying the electric field will have a direct effect on the adatom concentration gradient, thus allowing manipulation of the antiband formation.

When the applied electric field is reduced below critical (E_{cr}), the electromigration force is no longer sufficient to initiate the coarsening step-bunching process characterized by the gradual growth of step-bunch heights and terrace width with the annealing time. Determining E_{cr} is essential because it is related to the fundamental thermodynamic quantity $g(T)$, which is associated with the contribution of step-step repulsion to the surface free energy $f(\rho)$ of vicinal crystal surfaces given by^{13–16}

$$f(\rho) = f(0) + k\rho + g\rho^3, \quad (2)$$

where ρ is the density of steps. It should also be intuitive that a repulsive interstep interaction would necessitate a stronger critical field to induce the step-bunching process on surfaces with a reduced initial interstep distance l , which can be determined by the surface's overall miscut angle α from a low-index surface. Existing theoretical models provide different relationships between E_{cr} and l , depending on the sublimation conditions on the surface.¹⁷ Investigating the

$E_{\text{cr}}(l)$ dependency and comparing it to theoretical predictions would provide valuable information about the sublimation mechanism responsible for the development of step-bunching instability on Si(111).

Studies of vicinal Si(111) are often primarily concerned with the earlier stages of the step-bunching instability,⁶ which is induced by the maximum attainable electric field applied along the miscut direction. Consequently, despite extensive experimental and theoretical work, few advances have been made in understanding the phenomena that arise on surfaces subjected to extended annealing. Experimental data available on E_{cr} to date are also very limited,^{18,19} and their dependence on the initial interstep distance and sublimation temperature remains unknown. Here we study experimentally the development of the antiband instability under the influence of the reduced electromigration field. We were able to study morphologies of step-bunched surfaces at the onset stage of antiband formation, created by annealing with moderated E . We were able to test the relationship between the terrace width, the electromigration field, and the onset of antiband formation predicted by theoretical studies. Also, we systematically measure values of E_{cr} for Si(111) with different initial interstep distances l at 1130 °C (regime II) and 1270 °C (regime III) and compare measured $E_{\text{cr}}(l)$ dependences to the predictions of theoretical models.

II. EXPERIMENTAL PROCEDURE

We examined the onset of step bunching and antiband instabilities in Si(111) using a vacuum setup with a base pressure of 2×10^{-10} Torr, which combines independently controlled dc current and irradiative heating.¹⁸ The setup uses a heating shroud, supplied by an empty effusion cell, into which a dc-current annealing sample stage is inserted. The sample temperature is extracted from the sample's resistance, using silicon's large negative temperature coefficient for electrical resistivity. The capacity to decouple the dc-current heating from the sample temperature enabled us to control the strength of the electric field while maintaining the sample at a desired temperature. The strongest electric field was obtained when the dc current was the only source of heating during annealing while the minimum applicable field was determined by E_{cr} .

Rectangular 20×1.3 mm² samples were diced from n -type doped 0.525-mm-thick Si(111) wafers, with the misorientation angles α in the range 1.1–4° toward the [11-2] direction and the long sides of the samples aligned to the miscut direction. As will be demonstrated later in this paper, E_{cr} is weaker for Si(111) with lower α ; therefore the surface with the miscut angle of $\alpha = 1.1^\circ$ was selected to study the antiband formation as it provided a wide range of E over which the onset of antibands could be studied. Each sample was irradiatively heated and outgassed in a crucible for 24 h at 700 °C. To reduce surface defects the samples were then subjected to a mild 24 hour dc-current annealing at a temperature of approximately 450–500 °C. This was followed by repeated flash annealing up to 1250 °C for 10 s using dc current. In order to study the antiband formation, samples were annealed for time intervals ranging between 15 and 60 min at a temperature of 1270 °C with current driven in the step-down direction sufficient to induce the bunching morphology. Annealing at

1270 °C (regime III) was chosen as the antiband instability develops relatively rapidly at this temperature compared to other temperature regimes, at the high rate of step bunching of approximately 1 step/s.²⁰ Longer annealing times were used for samples annealed with weaker electric fields.

When studying the $E_{cr}(l)$ dependence, samples of different misorientation angles were annealed at 1130 °C (regime II) for 12 h with current in the step-up direction and 1270 °C (regime III) for 6 min with current in the step-down direction. The extent of carbon and oxygen contamination on the Si surface was determined in a separate experiment by Auger electron spectroscopy analysis, which showed that after flash annealing to 1250 °C the surface was free from carbon and oxygen contamination and remained clean after annealing for 12 h at 1130 °C.¹⁸ After the annealing sequence the samples were maintained at 650 °C for an hour using only irradiative heating. Finally, the samples were removed from vacuum, and the surfaces were analyzed *ex situ* using atomic force microscopy (AFM).

III. RESULTS AND DISCUSSION

Figure 2 shows surface morphologies formed on Si(111) with a misorientation of 1.1° toward the [11-2] direction as a result of extended annealing at 1270 °C with different applied electric fields. Normally, two samples were annealed with the same electric field. Annealing Si(111) for 15 min by dc current only ($E = 3.6$ V/cm) created morphology

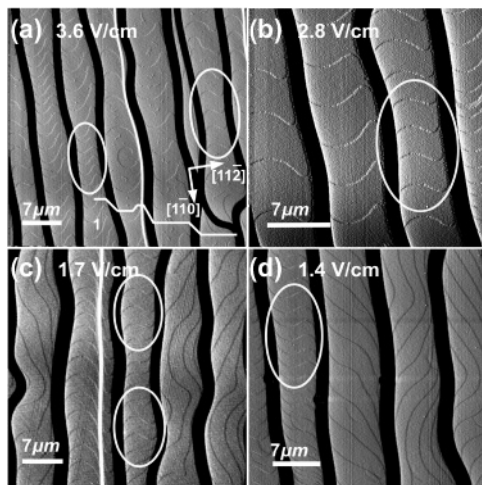


FIG. 2. Surface morphologies created on Si(111) by extended annealing at 1270 °C with different electric fields applied in the step-down direction. The step bunches are aligned along the [1-10] direction, while the down-step [11-2] direction is toward the right in all images. For weakened electromigration fields, wider terrace widths were required to initiate development of the step-bunching instability. Circled are the terrace areas containing crossing steps in a steady-state symmetric S shape. (a) A derivative image of a surface annealed for 15 min with $E = 3.6$ V/cm and current $I = 3.8$ A. The crossing steps on the narrower sections of the terraces are less developed toward the antiband. (b) A derivative image of a sample annealed for 30 min with $E = 2.8$ V/cm ($I = 2.9$ A). (c) A derivative image of Si(111) annealed for 60 min with $E = 1.7$ V/cm ($I = 1.8$ A). (d) A derivative image of a sample annealed for 60 min with $E = 1.4$ V/cm ($I = 1.5$ A).

characterized by bunches of closely spaced steps separated by 3.5–5.5- μ m-wide terraces [Fig. 2(a)]. Although 15 min was the shortest annealing time used in the experiment, most crossing steps acquired an asymmetric shape beyond the steady-state S shape, indicating that they were progressing toward antiband formation. The importance of annealing times was evident from a sample annealed by dc current exclusively for 30 min, where the majority of terraces developed antibands by completion of the annealing time. The step bunches have a wavy structure, and as a result, crossing steps at different stages of their evolution could be observed on each terrace due to variations in terrace width. For example, crossing steps on wider sections of a terrace marked as 1 in Fig. 2(a) have clearly progressed beyond the antiband onset point, while those constricted into a narrower section are in the steady-state S shape and aligned to the [11-2] direction perpendicular to the step bunches.

For samples annealed with weakened electromigration fields, wider terraces were found to be necessary to initiate antiband formation [Figs. 2(b)–2(d)]. To allow for this, the longer annealing times t were used in order to create wider terraces, based on the known relationship $L \sim t^{1/2}$.²¹ In addition, moderation of electromigration field reduced the rate of step bunching further, extending the required annealing times. Thus for $E = 2.8$ V/cm the onset of antiband formation was achieved after 30-min annealing [Fig. 2(b)], while for $E = 1.7$ and 1.4 V/cm, 60-min annealing was used [Fig. 2(c) and 2(d), respectively]. Despite the extended annealing times and wider terraces created by weaker electric fields, the shape of most crossing steps did not progress to the steady state or further toward the antiband formation. In contrast to the surfaces annealed with the greater electric fields, the steps on most terraces either curved into a long S shape or failed to achieve a regular pattern and extended over a distance of tens of micrometers along the step bunches.

Crossing steps in the steady S shape spanning terrace segments of different widths were observed on all studied samples, with the maximum width up to 80% larger than the minimum. Qualitatively, this is in agreement with the inequality (1), which gives a necessary but insufficient condition for the onset of the antiband instability. Thus for a fixed value of E , the lower limit of this relationship is defined by the width of the narrowest terrace where the steady-state profile of crossing steps can be achieved. Figure 3 shows the width of the narrowest observed terrace segments containing crossing steps in the steady-state shape L_m plotted against electromigration field E . Figure 3 clearly demonstrates that the minimum terrace width required to initiate antiband formation progressively increases as the electric field is reduced. The shaded area in Fig. 3 indicates terraces where the minimum requirements for E and L are not satisfied and consequently the formation of antibands cannot be achieved. To attain a quantitative understanding, the $L_m(E)$ data were fitted with a power-law function, and the relationship $E = 40.5L_m^{-1.96 \pm 0.05}$ was obtained (for $[E] =$ V/cm and $[L_m] = \mu$ m), which is in good agreement with the theoretical relationship (1) predicting $E \sim L_m^{-2}$ dependence. Variation of the electromigration force in this theoretical study was achieved by changing the effective charge for a fixed value of applied electric field,¹² while the result in Fig. 3, obtained by actual variation of applied electric

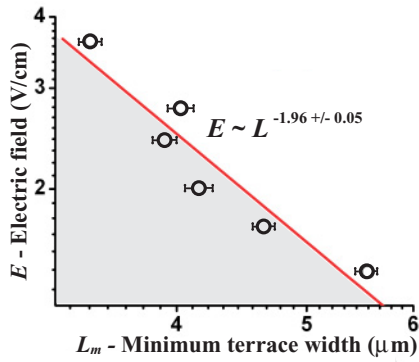


FIG. 3. (Color online) The width of the narrowest terrace segments containing crossing steps in the steady-state shape (L_m) vs electromigration field E , demonstrating the $E \sim L_m^{-2}$ dependence. The shaded area in the graph indicates terraces where the minimum requirements for E and L are not satisfied and, consequently, the formation of antibands cannot be achieved. The graph points obscure the error bars along the E axis. Ten to 15 sites of $50 \times 50 \mu\text{m}^2$ were randomly selected across the entire step-bunched area of each sample. The minimum width L_m was drawn from 30–40 separate terraces containing crossing steps in the steady-state S shape.

field, is experimental proof of the criteria for the onset of the antiband instability. Direct comparison of these relationships results in the numerical value of $2\tilde{\beta}a^2/q_{\text{eff}} = 40.5 \text{ V \AA}$. For $a = 0.3 \text{ nm}$ and the extrapolated value of $\tilde{\beta} = 28 \text{ meV/\AA}$,^{12,22,23} a value of the effective charge $q_{\text{eff}} = 0.012|e|$ can be estimated, where e is the elementary electric charge. This value is lower than $q_{\text{eff}} = (0.13\text{--}0.35)|e|$ obtained in previous experimental studies^{6,12,20} but is close to $0.02|e|$ deduced from first-principles calculations.²⁴

The minimum limit of the electromigration field in the study of antiband formation was determined by the critical field E_{cr} , as applying an electric field weaker than E_{cr} resulted in the cessation of the step-bunching process. Figure 4 shows morphological changes on a vicinal Si(111) when the electric field applied throughout the annealing process is reduced from the attainable maximum to critical. The surface produced by exclusively direct current heating (maximum attainable E) is characterized mostly by wide ($2\text{--}4 \mu\text{m}$ wide) terraces separated by narrow (approximately $1.0 \mu\text{m}$ wide) step bunches [Fig. 4(a)]. Annealing with weaker applied electric fields increases the interstep distance and thus results in the formation of wider step bunches, broadening at the expense of terraces and eventually accounting for most of the surface area [Fig. 4(b)]. Upon annealing with an electromigration field close to critical, the step bunches expand as far as the neighboring bunches, while relatively narrow, less than $1 \mu\text{m}$ wide, terraces can be still observed in some areas [Fig. 4(c)]. Annealing with the critical electric field E_{cr} or weaker fields results in the formation of a compressed step-density wave, where the number of atomic steps is relatively small compared to the coarsening step bunches and is not affected by the duration of annealing [Fig. 4(d)].

Values of E_{cr} were determined for samples of different miscut angles α at 1130 and 1270 °C (regimes II and III, respectively) and plotted as a function of the initial average interstep distance l (Fig. 5). Figure 5 clearly shows that in both

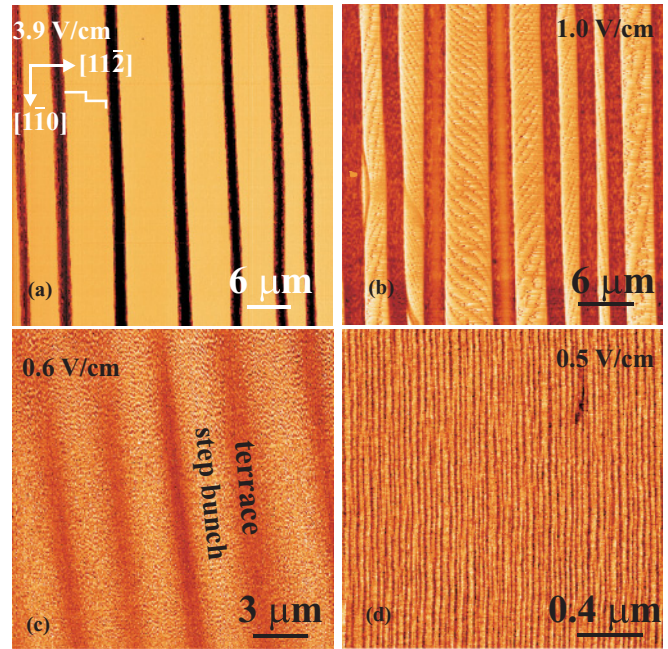


FIG. 4. (Color online) The step-bunching morphology on a Si(111) surface created at 1130 °C by annealing with different electromigration fields. The surface is off cut 2° toward the $[11\text{--}2]$ direction. The direction of the miscut is from left to right in all images, as shown by a stairway symbol in Fig. 4(a). Darker areas correspond to step bunches. (a) Phase AFM image of a step-bunched Si(111) surface obtained entirely by dc annealing with $E = 3.9 \text{ V/cm}$. (b) Phase AFM image of Si(111) after annealing with $E = 1.0 \text{ V/cm}$. (c) Phase AFM image demonstrating that the step bunches expand and occupy most of the surface after annealing at $E = 0.6 \text{ V/cm}$. (d) Phase AFM image of Si(111) after annealing with $E = 0.5 \text{ V/cm}$; the applied electric field is below critical and is insufficient to initiate the step-bunching process.

temperature regimes, reducing l results in a stronger interstep repulsive interaction, and a notable increase in the applied electric field is required to initiate the step-bunching process. Furthermore, increasing temperature from 1130 to 1270 °C increases E_{cr} by a factor of 2.3–3.3. Such a dramatic increase could be the result of different step-bunching mechanisms operating in the second and third temperature intervals, with the applied electric field being more effective in the second regime as a driving force for the instability. The enhanced interstep repulsive interaction arising from changes in the step morphology cannot be excluded. Fitting $E_{\text{cr}}(l)$ data with a power law shows that E_{cr} depends differently on l in the two investigated temperature intervals. While in regime II (1130 °C) $E_{\text{cr}}(l)$ follows a dependence that is close to $1/\sqrt{l}$, a relationship close to $E_{\text{cr}} \sim 1/l$ was observed in regime III (1270 °C).

While the $E_{\text{cr}} \sim 1/\sqrt{l}$ relationship is not well understood at this point, the $E_{\text{cr}} \sim 1/l$ dependence in temperature regime III can be explained within the framework of existing theories of step bunching. Generally, crystal sublimation involves two groups of processes. The first group includes surface diffusion accompanied by adatom desorption on terraces separated by atomic steps. The second group includes the interaction of adatoms with the atomic steps, i.e., attachment to the step edges, migration along the edges to the kink sites, detachment

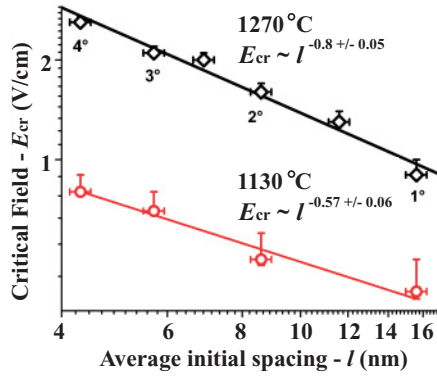


FIG. 5. (Color online) Dependence of the critical electric field E_{cr} on the initial average interstep distance l at 1130 and 1270 °C (temperature regimes II and III, respectively). The annotated angles next to experimental points indicate the corresponding degree of miscut off the Si(111) plane in the [11-2] direction. Some error bars are obscured by the graph points.

from the kink positions, and detachment from the steps. Depending on the relative rates of these processes, there are two distinguished sublimation regimes in the third temperature interval. First, the attachment-limited regime is characterized by relatively slow adatom attachment-detachment kinetics and fast diffusion on terraces. Second, the diffusion-limited regime is characterized by relatively slow surface adatom diffusion and fast kinetics at the steps. Sublimation proceeds differently in these regimes; therefore they should be considered and analyzed independently, and results should be compared with the experiment. For both regimes, the stability of a vicinal surface with respect to the unavoidable fluctuations in the step density is determined by the sign of the parameter $s = B_2 q^2 - B_4 q^4$, where q is the wave number of the Fourier mode.^{13,14,17} For small wave numbers the sign of s is determined by the sign of B_2 . The surface is unstable for $B_2 > 0$, i.e., the fluctuations in the distribution of the interstep distances grow with the sublimation time, while for $B_2 < 0$, the amplitude of the fluctuations decreases, indicating that the surface is stable.

In the case of attachment-detachment-limited sublimation (fast diffusion on terraces), the linear stability analysis gives^{13,17,25}

$$B_2 = -\frac{n_s^e \Omega}{2d_s} \left[v_{\text{drift}} + V_{cr} \frac{d_s}{K \tau_s} \right], \quad (3)$$

where n_s^e is the adatom surface equilibrium concentration, Ω is the area of one atomic site, and τ_s is the adatom's average lifetime in the state of mobile adsorption. Here $d_s = D_s/K$ is the characteristic length, where D_s is the adatom surface diffusion coefficient and K is the step kinetic coefficient. The adatom drift velocity is given by the equation $v_{\text{drift}} = q_{\text{eff}} E D_s / k_B T$, where k_B is Boltzmann's constant and T is absolute temperature. $V_{cr} = 12K\Omega g / k_B T l^3$ has units of velocity and characterizes the step-step repulsion. The surface becomes unstable ($B_2 > 0$) when the drift velocity v_{drift} is negative (i.e., adatom electromigration is in the down-step direction) and its absolute value is larger than the second

term in the square brackets in the Eq. (3). Thus, the onset of step-bunching instability is determined by the condition

$$v_{\text{drift}} + V_{cr} \frac{d_s}{K \tau_s} = 0, \quad (4)$$

which results in the equation for the absolute value of critical electromigration field E_{cr} :

$$|E_{cr}| = \frac{12\Omega g}{K q_{\text{eff}} \tau_s l^3}. \quad (5)$$

Clearly, this relationship between the critical field and the initial interstep distance is too strong to account for the experimentally observed $E_{cr} \sim 1/l$ dependence. However, in the limit of slow surface diffusion, the equations of step motion are different, and linear stability analysis of these equations gives¹⁷

$$B_2 = -\frac{d_s}{l^2} n_s^e \Omega \left[v_{\text{drift}} + V_{cr} \alpha^2 \frac{l^2}{\lambda_s^2} \right], \quad (6)$$

where λ_s is the adatom's mean diffusion path and $\alpha = \sqrt{1 + (q_{\text{eff}} E \lambda_s / 2kT)^2} \approx 1$. An equation for absolute value of E_{cr} can be obtained in the same way as before, resulting in

$$|E_{cr}| = \frac{12\Omega g}{d_s \lambda_s^2 q_{\text{eff}} l}. \quad (7)$$

Qualitatively, this dependence is in agreement with the experimentally observed $E_{cr} \sim 1/l$ relationship, indicating that in temperature interval III (1270 °C in our case), the sublimation process is diffusion limited and characterized by relatively slow surface adatom diffusion and fast kinetics at the atomic steps. The same conclusion was drawn in another experimental study from the relationship between the initial terrace width and the minimum terrace width within step bunches.²⁵ It is essential to point out that Eq. (1), which specifies the criteria for an onset of the antiband instability, was derived for the case of attachment-detachment-limited kinetics.¹² Theoretical analysis of antiband formation under the conditions of diffusion-limited sublimation is not available to date; therefore the question of the sublimation regime in the third temperature interval remains open and will be a subject of further investigation.

In the diffusion-limited regime the characteristic length d_s is smaller than l , and its lower limit is determined by the atomic distance a on a crystal surface.²⁵ Thus, for a quantitative estimate we can substitute into Eq. (7) $d_s = a = 0.3$ nm, $\Omega = a^2$, $g = 0.34$ eVnm,^{20,26} $\lambda_s = 10$ μm ,^{6,20,27} $l = 8.6$ nm (a miscut angle $\alpha = 2^\circ$), and $q_{\text{eff}} = 0.012|e|$, as obtained from studying antibands. The obtained value of $E_{cr} = 1.4$ V/cm is in good agreement with the value of $E_{cr} = 1.6$ V/cm experimentally measured for the sample with the same miscut of 2° .

IV. CONCLUSIONS

We created step-bunch morphologies on Si(111) by prolonged annealing at 1270 °C and investigated the effects of annealing with a reduced electromigration field on the evolution of terraces' crossing steps toward antiband formation. The relationship between the minimum terrace width L_m required for the antibands onset and the applied electromigration field E was investigated. A scaling relationship close to $E \sim L_m^{-2}$ was

measured, in accordance with the predictions of the existing theoretical model.

Values of the critical field E_{cr} , i.e., the minimum electromigration field required to initiate the step-bunching process, were measured for samples with different misorientation angles toward the [11-2] direction at 1130 and 1270 °C (regimes II and III, respectively) and were plotted as a function of the average initial interstep distance l . Reducing l resulted in a stronger interstep repulsive interaction and a notable increase in the applied electric field, required to initiate the step-bunching process. Moreover, increasing temperature from 1130 to 1270 °C increased E_{cr} by approximately a factor of 3. The $E_{cr}(l)$ dependence was found to be different in the two investigated temperature intervals. A relationship close to $E_{cr}(l) \sim 1/\sqrt{l}$ was measured for regime II, while a stronger

dependence close to $E_{cr} \sim 1/l$ was observed for regime III. The $E_{cr} \sim 1/l$ dependence provided strong evidence that adatom transport in temperature regime III is diffusion limited and characterized by relatively slow surface adatom diffusion and fast kinetics at the atomic steps. However, the question of the sublimation regime in the third temperature interval remains open. Good agreement was found between measured values of E_{cr} and values estimated using the analytical expression derived for the case of sublimation with the slow diffusion.

ACKNOWLEDGMENT

The financial support of Science Foundation Ireland, Contract No. 06-IN.1/191, is gratefully acknowledged.

*usovv@tcd.ie

¹J. Krug, in *Multiscale Modeling in Epitaxial Growth*, edited by A. Voigt, International Series of Numerical Mathematics, Vol. 149 (Birkhauser, Verlag, 2005) p. 69.

²I. V. Shvets, H. C. Wu, V. Usov, F. Cuccureddu, S. K. Arora, and S. Murphy, *Appl. Phys. Lett.* **92**, 023107 (2008).

³F. Cuccureddu, V. Usov, S. Murphy, C. O Coileain, and I. V. Shvets, *Rev. Sci. Instrum.* **79**, 053907, (2008).

⁴A. Latyshev, A. Aseev, A. Krasilnikov, and S. Stenin, *Surf. Sci.* **213**, 157 (1989).

⁵S. Stoyanov and V. Tonchev, *Phys. Rev. B* **58**, 1590 (1998).

⁶K. Fujita, M. Ichikawa, and S. Stoyanov, *Phys. Rev. B* **60**, 16006 (1999).

⁷F. Leroy, D. Karashanova, M. Dufay, J. M. Debierre, T. Frisch, J. J. Métois, and P. Müller, *Surf. Sci.* **603**, 507 (2009).

⁸M. Degawa, H. Minoda, Y. Tanishiro, and K. Yagi, *Surf. Sci.* **461**, L528 (2000).

⁹A. Latyshev, A. Krasilnikov, and A. Aseev, *Surf. Sci.* **311**, 395 (1994).

¹⁰D. J. Liu, J. D. Weeks, and D. Kandel, *Phys. Rev. Lett.* **81**, 2743 (1998).

¹¹J. Krug, V. Tonchev, S. Stoyanov, and A. Pimpinelli, *Phys. Rev. B* **71**, 045412 (2005).

¹²K. Thurmer, D. Liu, E. D. Williams, and J. D. Weeks, *Phys. Rev. Lett.* **83**, 5531 (1999).

¹³B. Ranguelov and S. Stoyanov, *Phys. Rev. B* **77**, 205406 (2008).

¹⁴B. Ranguelov and S. Stoyanov, *Surf. Sci.* **603**, 2907 (2009).

¹⁵P. Nozieres, *J. Phys. (Paris)* **48**, 1605 (1987).

¹⁶H. Jeong and E. D. Williams, *Surf. Sci. Rep.* **34**, 171 (1999).

¹⁷S. Stoyanov, in *Nanophenomena at Surfaces*, edited by M. Michailov, Springer Series in Surface Sciences, Vol. 47 (Springer, Berlin, 2011) p. 253.

¹⁸V. Usov, C. O Coileain, and I. V. Shvets, *Phys. Rev. B* **82**, 153301 (2010).

¹⁹V. Usov, C. O Coileain, and I. V. Shvets, *Phys. Rev. B* **83**, 155321 (2011).

²⁰Y. Homma and N. Aizawa, *Phys. Rev. B* **62**, 8323 (2000).

²¹D. J. Liu and J. D. Weeks, *Phys. Rev. B* **57**, 14891 (1998).

²²K. Sudoh, T. Yoshinobu, H. Iwasaki, and E. D. Williams, *Phys. Rev. Lett.* **80**, 5152 (1998).

²³J. M. Bermond, J. J. Métois, J. C. Heyraud, and F. Floret, *Surf. Sci.* **416**, 430 (1998).

²⁴D. Kandel and E. Kaxiras, *Phys. Rev. Lett.* **76**, 1114 (1996).

²⁵B. J. Gibbons, S. Schaepe, and J. P. Pelz, *Surf. Sci.* **600**, 2417 (2006).

²⁶N. Akutsu and Y. Akutsu, *J. Phys. Condens. Matter* **11**, 6635 (1999).

²⁷P. Finnie and Y. Homma, *Phys. Rev. Lett.* **82**, 2737 (1999).